

V. MICROWAVE ELECTRONICS*

Prof. L. D. Smullin
Prof. H. A. Haus
Prof. A. Bers

Prof. L. J. Chu
L. C. Bahiana
R. J. Briggs

D. Parker
A. Poeltinger
J. J. Uebbing

A. HIGH-PERVEANCE HOLLOW ELECTRON-BEAM STUDY

Direct-current measurements of the cylindrical cathode magnetron gun described in the previous report¹ have been completed. The beam-testing system that was used is shown schematically in Fig. V-1. The gun geometry, which is shown in Fig. V-2, was changed during the experiments by moving the anode with respect to the cathode. A reference coordinate system for determining the anode position is indicated in Fig. V-2. The beam cross section was observed on a carbon mesh screen, situated approximately 20 cm from the front end of the anode, which was movable over a distance of 2 cm. In all of the measurements the gun was in a uniform magnetic field with a flux density ranging up to $B = 2000$ gauss. The gun was operated with 1- μ sec pulses for voltages up to $V_o = 10$ kv. Voltage and current waveforms were measured on an oscilloscope. The current collected by the anode was measured separately, whereas the current intercepted by the mesh was measured together with the collector current and designated as beam current, I_b . The cathode current was also checked, and it was found always to be equal to the sum of anode and beam currents, i. e., there was no interception on the drift tube between the anode and the mesh.

In Figs. V-3 and V-4 the beam perveance $K = I_b/V_o^{3/2}$ is plotted against the magnetic field. The anode interception current is not shown in these graphs because there were too few measured points to draw significant curves. However, the general behavior of the interception for all combinations of parameters was such that at the left of the maxima of the perveance curves the interception would increase rapidly and the beam current would go down correspondingly, while at the right of these maxima the interception was negligible. Figure V-3 shows the influence of the gun geometry (anode position) on the maximum perveance and the increase of magnetic field that is required to operate the gun without excessive interception, i. e., near or at the right of the maxima of the curves. Figure V-4 shows the behavior of three typical fixed gun configurations with the voltage as a parameter. It is interesting to note that the maximum perveance for a fixed geometry is very nearly the same for all voltages. It can also be observed that the scaling law of the equations of motion, $K = \text{constant } V_o^{1/2}/B$, holds very closely for the middle curves in Fig. V-4, whereas there are considerable deviations from this

*This work was supported in part by the U. S. Navy (Office of Naval Research) under Contract Nonr-1841(49); and in part by Purchase Order DDL B-00337 with Lincoln Laboratory, a center for research operated by Massachusetts Institute of Technology with the joint support of the U.S. Army, Navy, and Air Force under Air Force Contract AF19(604)-7400.

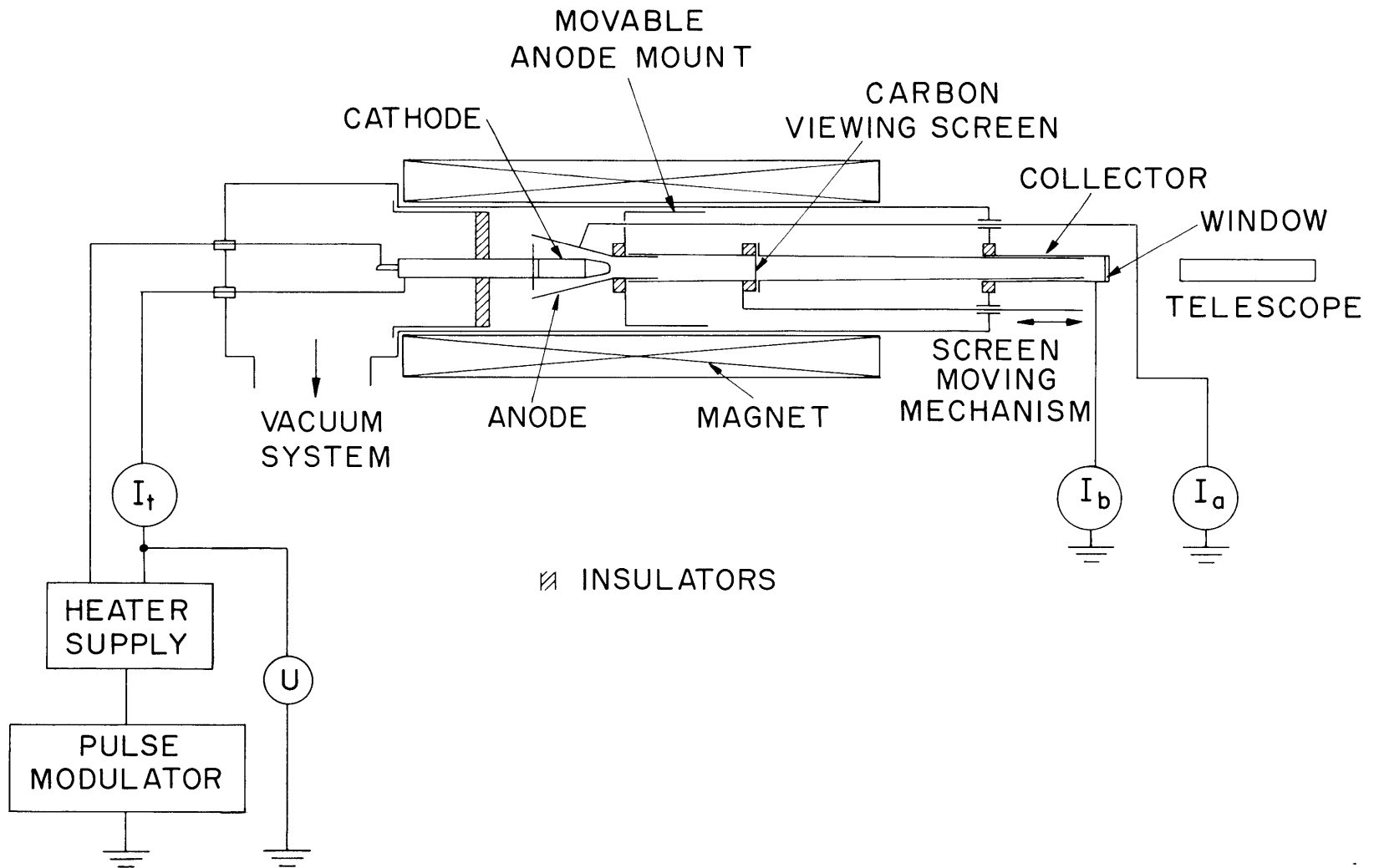


Fig. V-1. Beam-testing system.

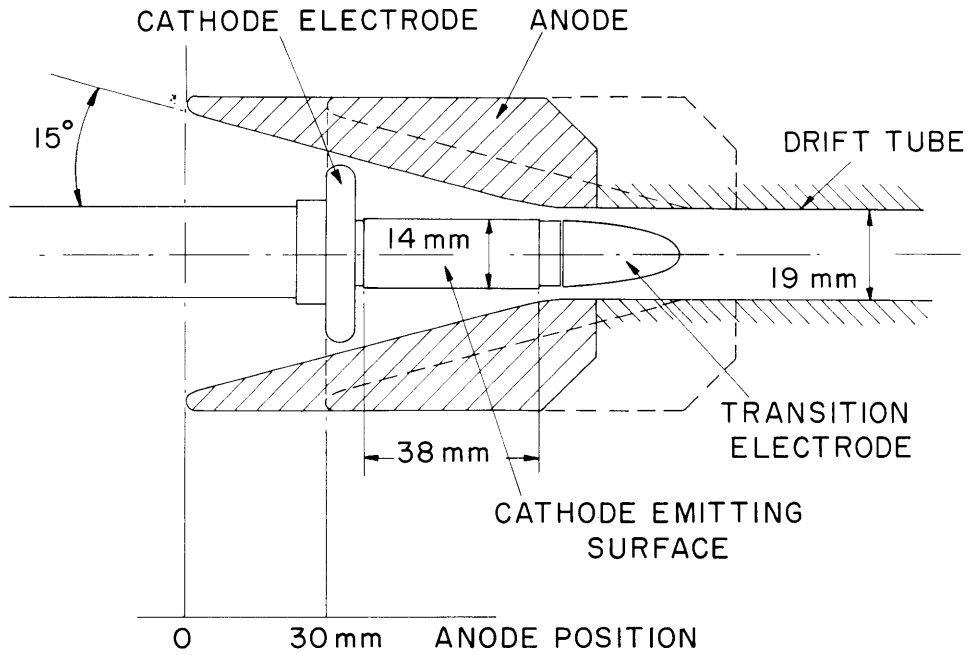


Fig. V-2. Cylindrical cathode magnetron gun.

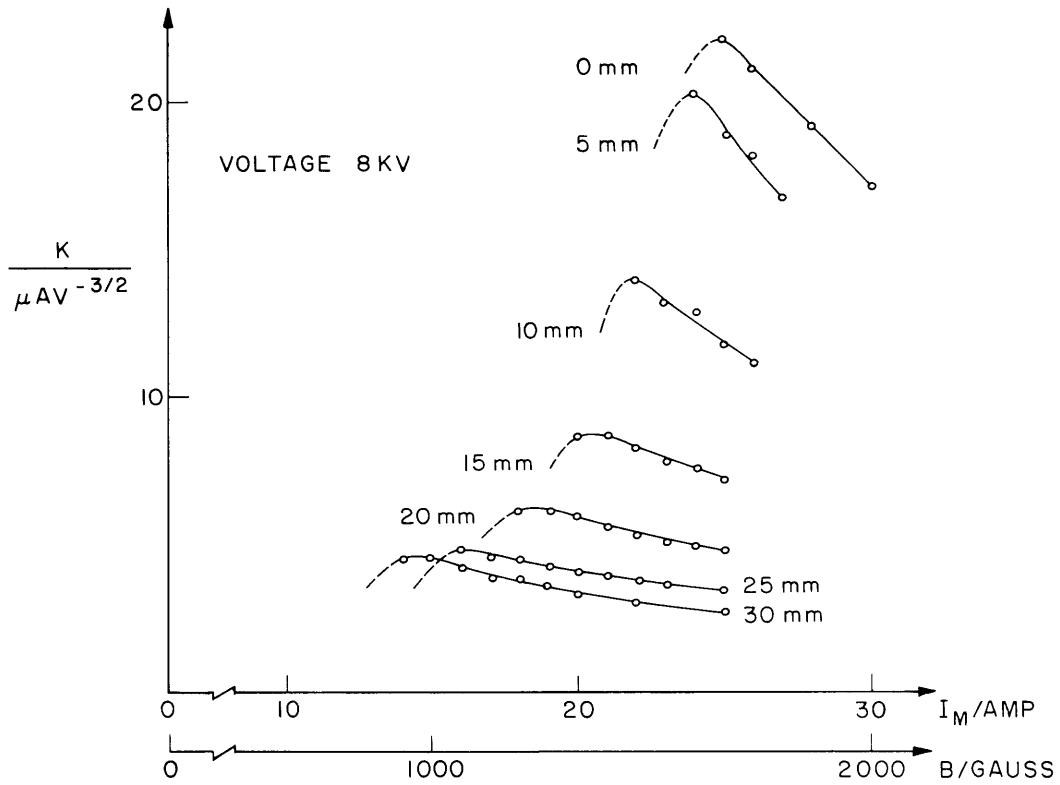


Fig. V-3. Beam perveance vs magnetic field for constant voltage and various anode positions as parameters.

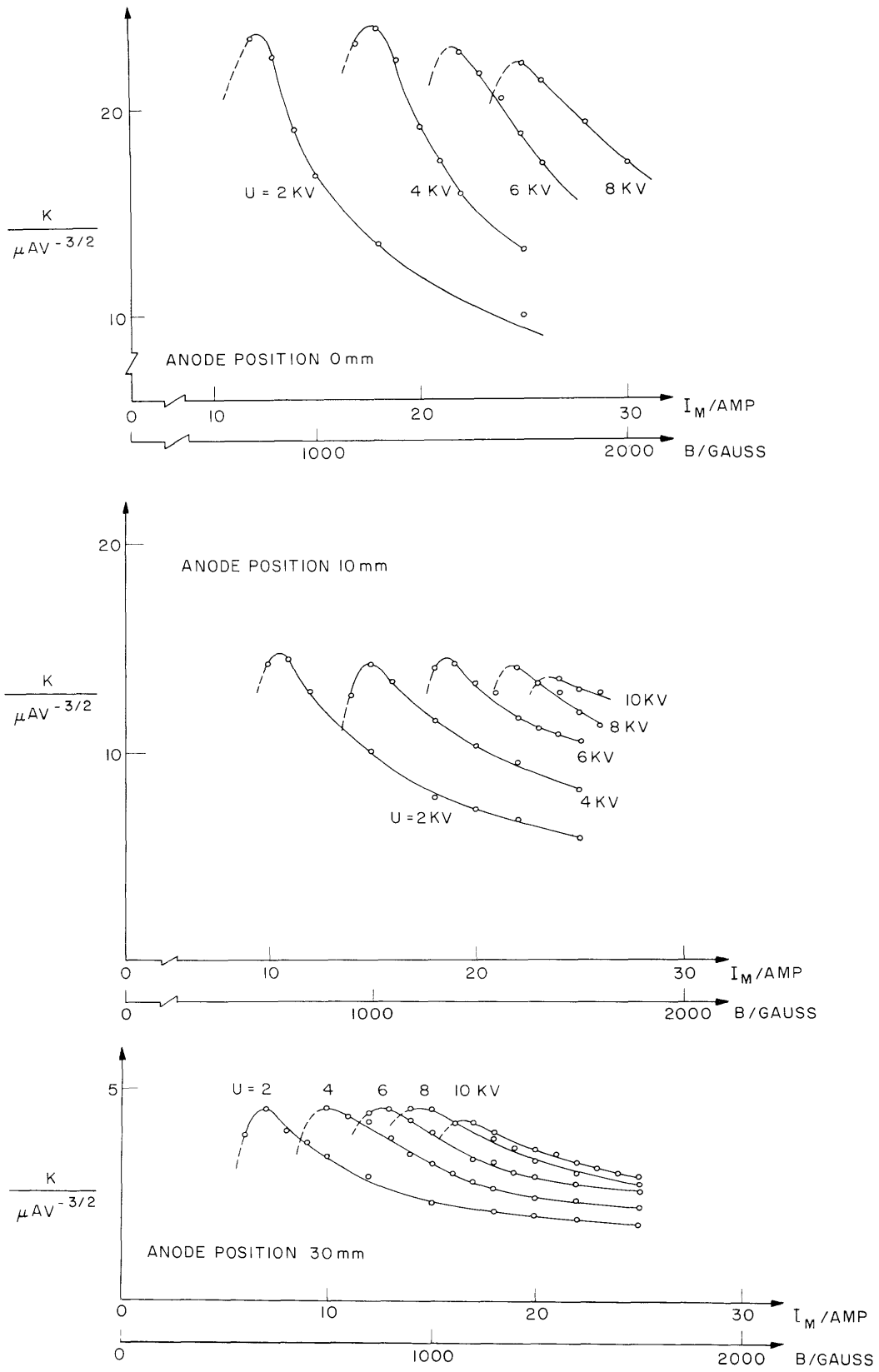


Fig. V-4. Beam perveance vs magnetic field.

scaling law for both extreme anode positions in the top and bottom curves. This seems to indicate that the electron flow for the intermediate position shown in the middle curves approximates a laminar flow. Other evidence for this fact was the observed beam cross section, which was more uniform for this configuration than for any other.

Generally, the beam cross sections were slightly asymmetric and a slight breakup into four equally spaced lobes was visible around the circumference at low average power (low pulse repetition rate). Over a beam length of approximately 2 cm no scalloping was detectable. The inner diameter of the beam was essentially the same as the cathode diameter. The thickness decreased with increased magnetic field, and was approximately in the range 0.7-1.5 mm (8-15 per cent). The range of plasma frequencies ($\omega_p^2 = e\rho/m\epsilon_0$) given by the various combinations of parameters extended to approximately 2000 mc. This value pertains to the approximately laminar beam obtained by using an anode position of 10 mm with a perveance of 13×10^{-6} amp/volt^{3/2} for a voltage of 10 kv and a magnetic flux density of 1650 gauss.

A. Poeltinger

References

1. A. Poeltinger, High-perveance hollow electron-beam study, Quarterly Progress Report No. 65, Research Laboratory of Electronics, M.I.T., April 15, 1962, p. 45.

B. KINEMATIC THEORY OF GAP INTERACTION FOR RELATIVISTIC ELECTRON BEAMS

The kinematic theory of gap interaction for electron beams having finite dimensions transverse to the direction of unperturbed flow was first given by Fremlin et al.¹ and by Warnecke and Guenard.² These authors assume that the unperturbed flow is non-relativistic and their theories are, therefore, restricted to electron beams having $v_0 \ll c$, where v_0 is the unperturbed electron velocity, and c is the velocity of light. For relativistic electron beams the correct gap interaction can be obtained from either a self-consistent kinematic theory or from the weak space-charge theory³ in the limit $(\omega_p/\omega) \rightarrow 0$. In this report we shall give these results for a cylindrical electron beam.

Consider the electron-beam waveguide shown in Fig. V-5 in which the gap opening in the perfectly conducting wall is short compared with a free-space wavelength and uniform in ϕ . The electric field in the gap opening can then be approximately specified from a quasistatic analysis. The electric field inside the waveguide can be written in Fourier form

$$E_z(r, z) = \frac{1}{2\pi} \int_{-\infty}^{\infty} \mathcal{E}(\beta) e^{j\beta z} dz. \quad (1)$$

(V. MICROWAVE ELECTRONICS)

Here, $\mathcal{E}(\beta)$ is determined by requiring that E_z satisfy Maxwell's equations and the boundary conditions, including the specified field at the gap opening in the wall. In the absence of space-charge fields (kinematic limit) this is the only field that acts on the electrons. We shall restrict our considerations to a confined-flow electron beam that has its motion constrained to the z-direction by a strong longitudinal magnetic field applied externally.

The gap interaction is most conveniently described by a linear three-port transformation among the beam modulations at the mid-plane of the gap and the circuit fields at the gap.⁴

$$\begin{bmatrix} U_+ \\ I_+ \\ I_g \end{bmatrix} = \begin{bmatrix} 1 & 0 & M \\ 0 & 1 & Y_o N \\ Y_o N & M & Y_{el} \end{bmatrix} \begin{bmatrix} U_- \\ I_- \\ V_g \end{bmatrix} \quad (2)$$

Here, U_- and I_- are the kinetic voltages and currents just preceding (-) and following (+) the mid-plane of the gap position,

$$V_g = \int_{-d}^d E_z(a, z) dz, \quad (3)$$

and I_g is the gap current defined so that $\frac{1}{2} V_g I_g^*$ is the complex power flow from the circuit to the electron-beam waveguide. The modulations in the electron beam which precede and follow the gap are obtained by applying the usual drift transformations to U_- , I_- , and U_+ , I_+ , respectively. The gap interaction for the entire span of circuit fields (in general, from $z = -\infty$ to $z = +\infty$) is contained in the elements of the matrix of Eq. 2.

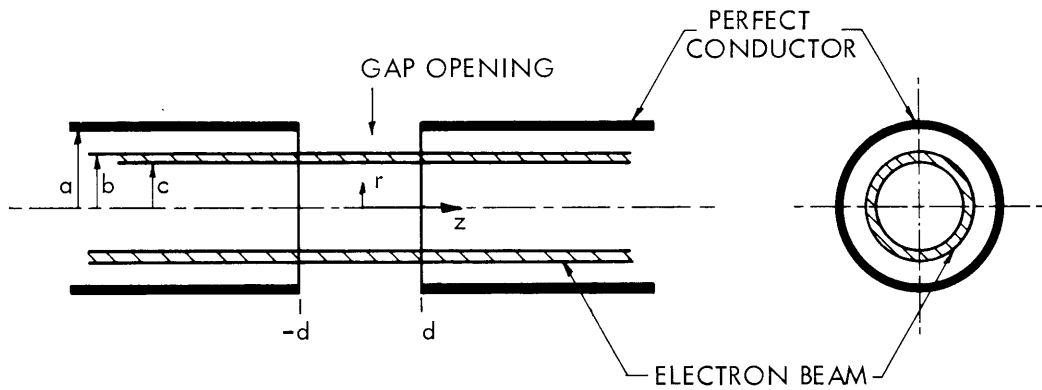


Fig. V-5. Electron-beam waveguide with gap.

(V. MICROWAVE ELECTRONICS)

For a ϕ -symmetric opening in a waveguide with thin walls that are closely spaced compared with the waveguide diameter, Eq. 1 gives⁴

$$\mathcal{E}(\beta) = \frac{I_0(\gamma r)}{I_0(\gamma a)} J_0(\beta d). \quad (4)$$

Here,

$$\gamma^2 = \beta^2 - k^2 \quad (5)$$

$$k = \frac{\omega}{c}, \quad (6)$$

J_0 is the ordinary Bessel function, and I_0 is the modified Bessel function. The evaluation of the matrix elements, by using the kinematic equations of motion for an electron stream at radius r , gives

$$M = \left[\mathcal{E}(\beta) \right]_{\beta = \beta_e} \quad (7)$$

$$Y_o N = \frac{G_o}{R(R+1)} \left[\frac{\partial \mathcal{E}(\beta x)}{\partial x} \right]_{\substack{x=1 \\ \beta = \beta_e}} \quad (8)$$

$$\text{Re } Y_{el} \equiv G_{el} = \text{Re } (Y_o N M). \quad (9)$$

Here,

$$\beta_e = \frac{\omega}{v_o}; \quad \gamma = \frac{\beta_e}{R} \quad (10)$$

$$G_o = \frac{I_o}{V_o} \quad (11)$$

$$R = 1 + \frac{V_o}{V_n}, \quad (12)$$

with I_o the unperturbed beam current, V_o the unperturbed beam voltage, and $V_n = 5.11 \times 10^5$ volts. The imaginary part of Y_{el} can only be given in terms of integrals⁴ involving $\mathcal{E}(\beta)$. Using Eqs. 4-12, we obtain

$$M = \frac{I_0(\gamma r)}{I_0(\gamma a)} J_0(\beta_e d) \quad (13)$$

$$Y_o N = \frac{G_o}{R(R+1)} M \left[R^2 \left(\gamma a \frac{I_1(\gamma a)}{I_0(\gamma a)} - \gamma r \frac{I_1(\gamma r)}{I_0(\gamma a)} \right) + \beta_e d \frac{J_1(\beta_e d)}{J_0(\beta_e d)} \right] \quad (14)$$

(V. MICROWAVE ELECTRONICS)

$$G_{el} = Y_o NM . \quad (15)$$

For a beam of finite transverse thickness the parameters of the gap matrix follow directly from either the weak space-charge theory³ or an average of Eqs. 13-15:

$$M = \frac{2[(\gamma b)I_1(\gamma b) - (\gamma c)I_1(\gamma c)]}{[(\gamma b)^2 - (\gamma c)^2] I_o(\gamma a)} J_o(\beta_e d) \quad (16)$$

$$Y_o N = \frac{G_o}{R(R+1)} M \left[R^2 \left(2 + \gamma a \frac{I_1(\gamma a)}{I_o(\gamma a)} - \frac{(\gamma b)^2 I_o(\gamma b) - (\gamma c)^2 I_o(\gamma c)}{(\gamma b)I_1(\gamma b) - (\gamma c)I_1(\gamma c)} \right) + \beta_e d \frac{J_1(\beta_e d)}{J_o(\beta_e d)} \right] \quad (17)$$

$$G_{el} = Y_o NM . \quad (18)$$

The well-known forms for the nonrelativistic limit are obtained by setting $R = 1$.

In the ultrarelativistic limit, for example, for interest in particle accelerators, we have

$$R \rightarrow \frac{V_o}{V_n} \gg 1 \quad (19)$$

$$v_o \rightarrow c \quad (20)$$

$$\beta_e \rightarrow k = \frac{\omega}{c} \quad (21)$$

$$\gamma \rightarrow \frac{k}{R} \rightarrow 0, \quad (22)$$

and the gap parameters of Eqs. 16-18 become

$$M \rightarrow J_o(kd) \quad (23)$$

$$Y_o N \rightarrow \frac{G_o}{R^2} M \left[\frac{(ka)^2}{2} + kd \frac{J_1(kd)}{J_o(kd)} \right] \quad (24)$$

$$G_{el} = Y_o NM . \quad (25)$$

Hence, for a fixed perveance $(I_o/V_o^{3/2})$ the current coupling and the electronic loading are proportional to $V_o^{-3/2}$.

A. Bers

References

1. J. H. Fremlin, A. W. Gent, D. P. R. Petrie, P. J. Wallis, S. T. Tomlin, Principles of velocity modulation, J. Inst. Elec. Engrs. (London) 93, 875 (1946).
2. R. Warnecke and P. Guenard, Les Tubes Électroniques à Commande par Modulation de Vitesse (Gauthier-Villars, Paris, 1951), p. 524.
3. A. Bers, Linear space-charge theory of gap interaction between an electron beam and electromagnetic fields, NTF, Bd. 22, 53-60 (1961).
4. A. Bers, Interaction of Electrons with Electromagnetic Fields of Gaps with Applications to Multicavity Klystrons, Sc.D. Thesis, Department of Electrical Engineering, M. I. T., 1959.

C. HOLLOW ELECTRON BEAMS FROM HOLLOW CATHODES

Previous work¹ has shown that the hollow cathode is a good source of high-density electron beams that appear to be hollow. For the usual form of cathode geometry, however, the emitted current has been found to decrease markedly upon application of an axial magnetic field.² In the present investigation a cylindrical hollow cathode was used, since this geometry would seem to be least affected by the magnetic field used for beam focusing.

A cylinder, 0.125 inch in diameter, internally coated with (Ba Sr)O, was used in all of our experiments. In the absence of a magnetic field, the beam as seen on a soot-coated collector was irregularly hollow, the exact pattern being determined by the state of activation of the different areas of the cathode from which electrons are emitted. The current varied widely as the activity of the cathode changed, and temperature dependence was always observed. For constant activation and temperature, the total emitted current was always found to vary linearly with the electric field in front of the cathode opening. Using an anode with a 0.21875-inch hole, spaced 0.08 inch from the cathode, we could obtain 30-ma hollow beams with 800 volts on the anode. The corresponding current density for an inner diameter that was two-thirds of the outer diameter was 0.7 amp/cm². When a magnetic field was applied, the beam became more uniformly hollow and the current decreased slightly — 20 per cent at 800 gauss. Because the electrons travel at an angle as great as 20° with respect to the tube axis, the beam is severely scalloped. Attempts at eliminating this scalloping with electrostatic lenses were unsuccessful.

In order to determine the cause of the large angular spread of the electrons, a tube was built with a grid that could be swung in front of the anode aperture to eliminate the diverging effect of the anode aperture fields. Figures V-6 and V-7 show beam diameter versus distance with and without the anode grid. Also plotted are the calculated electron trajectories for electrons emitted from different parts of the cathode, with space charge and initial velocities of the electrons neglected. The electric field was measured in an electrolytic tank. These curves indicate that most of the electrons come from the region near the lip of the cylinder and that the beam divergence is due primarily to the fields in the cathode itself, and secondarily to the anode aperture fields.

If the effects of magnetic field in the cathode region are neglected, it is quite easy to calculate the expected beam diameter versus magnetic field at a given distance down the axis of the tube. The calculated points are shown in Fig. V-8, together with experimental points. The measured injection angle was 11°. Also plotted are universal beam scalloping curves in which α is the injection angle, r_o , the cathode radius, r_e , the cyclotron radius; B , the magnetic field, and V_a is the anode accelerating voltage. These curves indicate that large magnetic fields will be necessary for a smooth beam. It may be possible to correct this beam divergence by means of carefully placed electrostatic

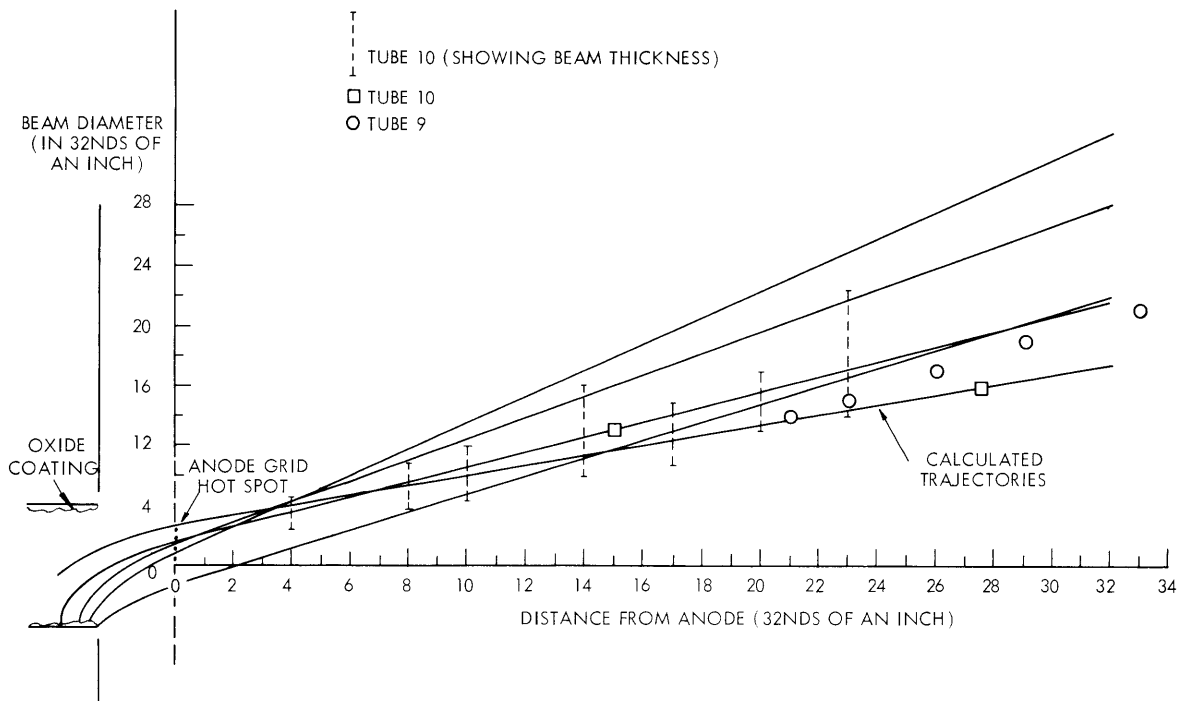


Fig. V-6. Beam diameter versus distance; anode grid in place; no magnetic field.

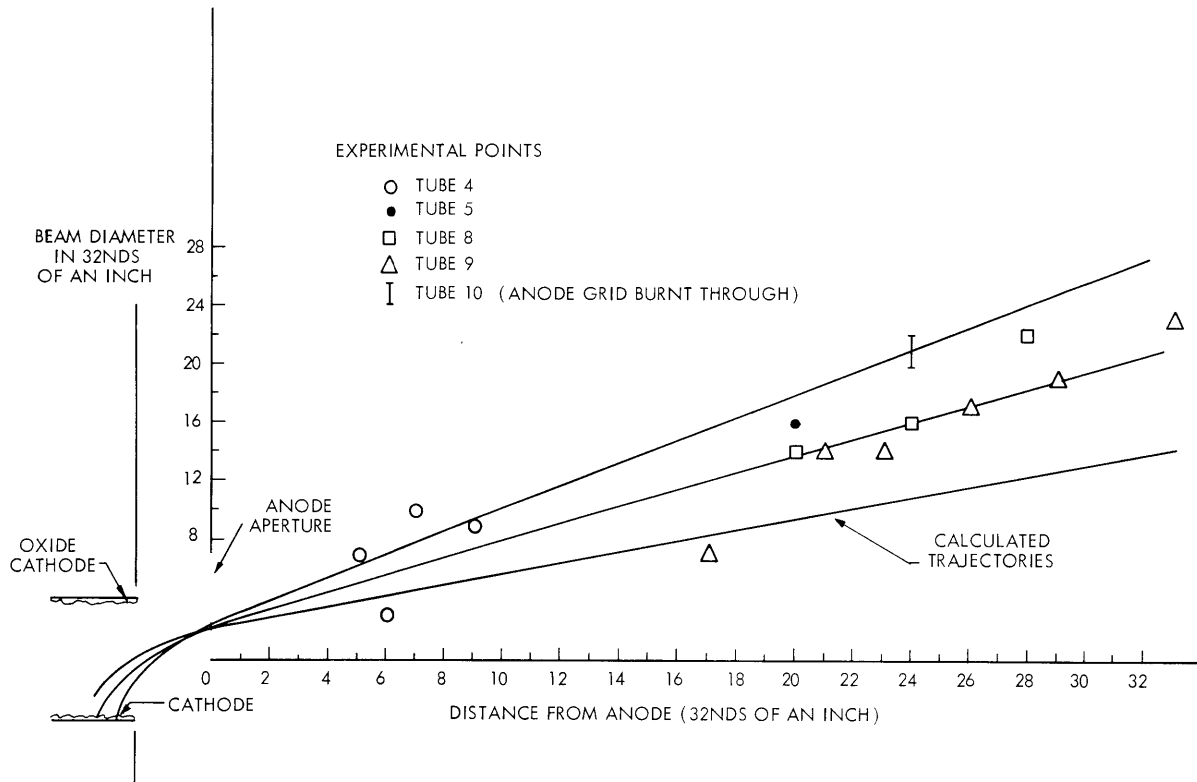


Fig. V-7. Beam diameter versus distance; no anode grid; no magnetic field.

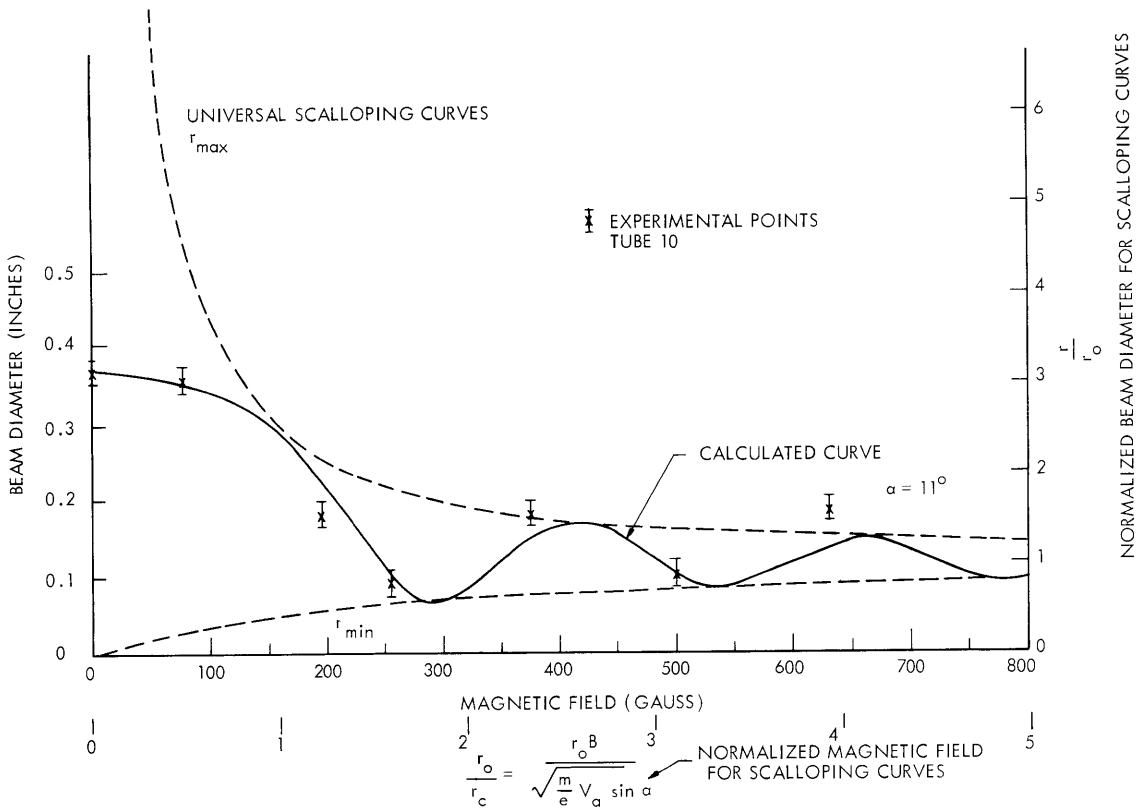


Fig. V-8. Beam diameter versus magnetic field at 15/64-inch anode-collector spacing.

lenses. In any event, the problem and its causes are now well demonstrated.

More details of this study are available in the author's thesis.³

J. J. Uebbing

References

1. H. Shelton, Quarterly Progress Report, Research Laboratory of Electronics, M.I.T., October 15, 1954, pp. 27-29.
2. H. Shelton, Quarterly Progress Report, Research Laboratory of Electronics, M.I.T., April 15, 1954, pp. 38-40.
3. J. Uebbing, Hollow Electron Beams from Hollow Cathodes, E.E. Thesis, Department of Electrical Engineering, M.I.T., May 21, 1962.

